Alexandria Engineering Journal (2013) xxx, xxx–xxx

Alexandria University

Alexandria Engineering Journal

www.elsevier.com/locate/aej
www.sciencedirect.com

ORIGINAL ARTICLE

Photocatalytic degradation of phenol and benzoic acid using zinc oxide powders prepared by the sol–gel process

Hadj Benhebal [a,*], Messaoud Chaib [a], Thierry Salmon [b], Jérémy Geens [b], Angélique Leonard [b], Stéphanie D. Lambert [b], Michel Crine [b], Benoît Heinrichs [b]

[a] Laboratoire de Chimie et Environnement, Université de Tiaret, BP 78 Zaaroura, Tiaret 14000, Algeria
[b] Laboratoire de Génie Chimique, B6a, Université de Liège, Liège B-4000, Belgium

Received 28 February 2011; revised 30 March 2013; accepted 16 April 2013

KEYWORDS

Photocatalysis
Phenol
Benzoic acid
Zinc oxide
Sol–gel

Abstract Photocatalytic degradation of phenol and benzoic acid in aqueous solution was studied using zinc oxide (ZnO) powder synthesized by sol–gel process. Synthesized catalyst was characterized by X-ray diffraction and transmission electron microscopy. The Brunauer–Emmett–Teller surface area, pHpzc, and the band gap of the catalyst samples were also measured. The influence of various key parameters such as amount of photocatalyst, initial solution pH, and the initial concentration of phenol and benzoic acid was investigated.

1. Introduction

Aromatic pollutants, in particular phenolic derivatives, constitute a group of organic pollutants that are often encountered in the environment as a result of their numerous applications. Phenolic derivatives are the products of many industrial processes, and they may be found in trace quantities in industrial wastewater. These compounds are considered as priority pollutants since they are harmful to organisms, and many of them have been classified as hazardous pollutants because of their potential to harm human health [1]. In recent years, many studies have been focused on the photocatalytic degradation of organic compounds by semiconductor particles acting as photocatalysts [2–4].

Heterogeneous photocatalytic reactions were studied for more than fifty years. If few publications have been published before, the mostly cited one is the one of Honda and Fujishima in 1972 [5]. The heterogeneous photocatalytic process is initiated when a photon with energy equal or greater than the band gap energy (E_{bg}) of the photocatalyst reaches its surface, resulting in the generation of mobile electrons in the higher energy conduction band (E_{cb}) and positive holes in the lower energy valence band (E_{vb}) of the catalyst. The photocatalytic reaction proceeds via a series of chemical events, through the utilization of both the electron–hole h^+ for oxidation processes and eventually to the capture of the e^- electron for reduction processes, as well as potential formation of super oxide anions and hydrogen peroxide from oxygen. These facts

* Corresponding author. Tel./fax: +213 46 45 20 63.
E-mail address: benhebalh@yahoo.fr (H. Benhebal).
Peer review under responsibility of Faculty of Engineering, Alexandria University.

Production and hosting by Elsevier

1110-0168 © 2013 Production and hosting by Elsevier B.V. on behalf of Faculty of Engineering, Alexandria University.
http://dx.doi.org/10.1016/j.aej.2013.04.005

allow both mineralization of organic species and removal of inorganic cations [6].

The photocatalytic activity of ZnO is almost similar to that of Titania, i.e., ZnO is found to be as reactive as TiO_2 under concentrated sunlight (as the band gap energy of ZnO is same as that of TiO_2, i.e., 3.2 eV). But in some cases, the photocatalytic activity of ZnO is considered to be less than that of TiO_2, due to photocorrosion tendency of ZnO. In aqueous solution, ZnO shows photocorrosion tendency with the illumination of UV light [7,8]

However, the photocatalytic activity of ZnO is limited to irradiation wavelengths in the UV region because ZnO semiconductor has a wide band gap of about 3.2 eV and can only absorb UV light with wavelengths below 387 nm [9]. It is particularly interesting to synthesize ZnO by the sol–gel process because sol–gel chemistry is an efficient tool for controlling morphology and reactivity of solids. In recent decades, it has permitted the development of new highly dispersed materials, presenting both good homogeneity and purity [10–12]. The efficiency of photocatalytic processes has been shown to depend on several different characteristics of the semiconductor particles, such as their surface properties, the position of their band gap potentials, and the mobility and recombination rate of the charge carriers generated by UV light absorption. Moreover, a relevant role is also played by the chemical and adsorption properties of the degradation substrate, depending also on experimental conditions, such as pH and the substrate to photocatalyst concentration ratio [13].

In this work, ZnO powder was synthesized by sol–gel method using zinc acetate dihydrate as a precursor and characterized by using techniques such as nitrogen adsorption isotherms, X-ray diffraction (XRD), scanning electron microscopy (SEM), and UV–Vis spectroscopy. Photocatalytic activity of catalyst was evaluated by measuring the photodegradation of phenol and benzoic acid. The effect of different operating conditions, such as catalyst loading, initial pH, and pollutant concentrations, was also studied.

2. Experimental section

2.1. Photocatalyst preparation

ZnO powder was prepared by sol–gel method from zinc acetate dihydrate, oxalic acid using ethanol as solvent. ZnO gel was obtained by dissolving 50.1 mmole of zinc acetate $(CH_3COO)_2Zn{\cdot}2H_2O$ in 300 ml ethanol (C_2H_6O) and refluxing at 60 °C under vigorous stirring for 30 min. 140 mmole of oxalic acid ($H_2C_2O_4$) was mixed with 200 ml of ethanol and added to the previous solution slowly. The final mixture was refluxed at 50 °C for 60 min before left cool down to room temperature. Finally, the ZnO gel was dried at 80 °C for 20 h (Xerogel), and the powder calcined under flowing air (0.1 mmol s^{-1}) for 4 h at 650 °C.

2.2. Photocatalyst characterization

Nitrogen adsorption–desorption isotherms were measured at −196 °C on a Fisons Sorptomatic 1990 after out gassing for 24 h at ambient temperature.

ZnO particles sizes were examined by SEM on a Jeol JSM-840 under high vacuum, at an acceleration voltage of 20 kV. The samples were deposited onto carbon tape and coated with gold in a Balzers plasma sputterer (30 s at 30 mA).

XRD was used to determine the nature and the size of crystalline phases of ZnO. Patterns were obtained with hand-pressed samples mounted on a Philips PW 1830 goniometer using the Cu Kα line (λ = 0.15458 nm).

Diffuse reflectance measurements in the UV/Vis region (250–800 nm) were performed on a Varian Cary 5000 UV/Vis/NIR spectrophotometer, equipped with a Varian External DRA-2500 integrating sphere, using $BaSO_4$ as the reference. Spectra were recorded in diffuse reflectance mode (R = reflection intensity) and were transformed into the absorbance coefficient ($F(R)$) by the Kubelka–Munk function, $F(R) = (1 - R)^2/2R$ [14]. ZnO band gap value, Eg, was obtained from the plot of the Kubelka–Munk function $(F(R)E)^{1/2}$ vs. the energy of the absorbed light, E [14,15].

By definition, pHpzc is the pH of the solution in contact with solid at which the net surface charge on the surface of an adsorbent particle is zero. The pHpzc of the zinc oxide was measured by the pH drift method [16]. The determination of pHpzc was done by adjusting the pH of 0.01 M NaCl (50 cm^3) to values between 1 and 10 obtained by adding either 0.1 M HCl or NaOH. About 0.05 g of zinc oxide was added into each solution at room temperature and then shaken for 48 h. The final pH was measured and plotted against the initial pH. The pH at which the plotted curve intersects the line of pH (final) = pH (initial) was taken as the pHpzc of the zinc oxide surface.

2.3. Photocatalytic experiments

To determine the photocatalytic activity of the synthesized material, the study of the degradation of phenol (Riedel-de Haën, 99.5%) and benzoic acid (Aldrich; Purity >99.5%) under UV irradiation was realized.

The phenol and benzoic acid degradation was carried out at 20 °C using a water-cooled cylindrical 200 mL glass reactor (Fig. 1), with external lamp (125 W UV lamps, Black light Mercury HgV). In a first time, the amount of catalyst powder, [ZnO], was kept at 0.1 g L^{-1}, the initial concentration of pollutant, C_0, was 0.2 g L^{-1}, and the pH of the solution was fixed to 6.5. In a second time, photocatalytic experiments were realized with varying operating variables: three different pH values (2.5, 6.5, and 12.5) adjusted with aqueous solutions of HCl and NaOH (2 mol L^{-1}), ten photocatalyst concentrations [ZnO] (from 0.5 to 2.5 g L^{-1}), and five initial concentrations of pollutant, C_0 (from 0.05 to 0.25 g L^{-1}).

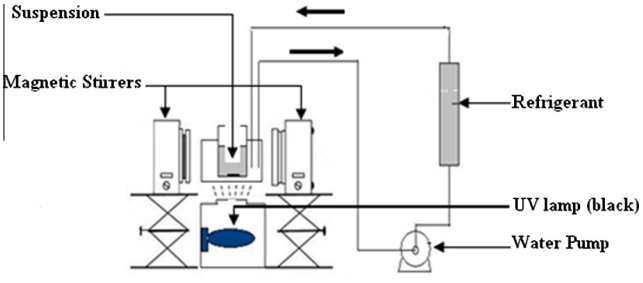

Figure 1 Reactor used in the photocatalytic experiments.

Please cite this article in press as: H. Benhebal et al., Photocatalytic degradation of phenol and benzoic acid using zinc oxide powders prepared by the sol–gel process, Alexandria Eng. J. (2013), http://dx.doi.org/10.1016/j.aej.2013.04.005

Before each photocatalytic test, the mixture was kept in the dark for 1 h to ensure that the adsorption–desorption equilibrium was reached before illumination. The sample was then taken out at the end of the dark adsorption period, just before the light was turned on, in order to determine the phenol and benzoic acid concentration in solution, C_0'. In all cases, the difference between C_0 and C_0' was found to be negligible when compared to the error of the method. When the lamp was turned on, the experiment started. After a given irradiation time, the sample was taken out from reactor; then, the catalyst [ZnO] was removed by centrifugation and the remaining phenol, and benzoic acid concentration in the solution was measured with the photocoulometric method of 4-amino-antipirine [17], analyzed with a 1201 Shimadzu spectrophotometer.

Repetition tests were made to ensure the reproducibility of results. So, all the photocatalytic results presented in this work are the mean of three replicates.

3. Results and discussion

3.1. Characterization of crystallized pure ZnO powder by the sol–gel process

Fig. 2 shows the XRD patterns of ZnO nanocrystalline powder. The sharp intense peaks of ZnO confirms the good crystalline nature of ZnO and the peaks originated from (100), (002), (101), (102), (110), (103), (200), (112), and (201) can be indexed as a hexagonal wurtzite ZnO structure which are consistent with the values in the standard card (JCPDS 36-145)[18]. No diffraction patterns from any other impurities were detected, which confirms that the synthesized powder was pure ZnO hexagonal. Crystallite size "D" was obtained by measurements of the broadening of diffraction lines and applying the Debye–Scherrer formula [19].

$$D = 0.9\lambda/\beta\cos\theta \quad \text{(I)}$$

where λ is the wavelength of Cu Ka radiations (1.54 Å), b the full width at half-maximum of the peak corresponding to the plane (101), and θ the angle obtained from 2θ value corresponding to maximum intensity peak in XRD pattern. The diameter of crystallite size of synthesized ZnO powder was 20 nm.

By SEM analysis, it is observed in Fig. 3 that the calcined ZnO powder is composed of aggregates of ZnO particles. All of the particles are uniform, spherically shaped.

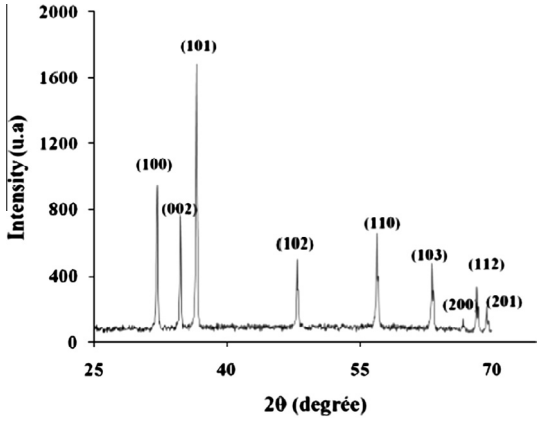

Figure 2 XRD pattern of the calcined ZnO powder.

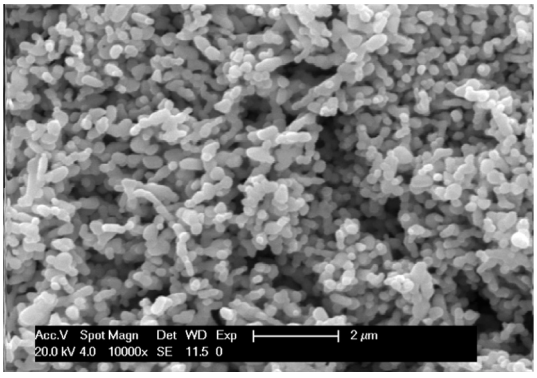

Figure 3 SEM micrograph of the calcined ZnO powder.

A nitrogen adsorption–desorption isotherm was carried out to analyze the textural properties of the calcined ZnO powder, and it is presented in Fig. 4. This isotherm displays a slight increase in the adsorbed volume at very small p/p_0 values, which is characteristic of the presence of micropores (< 2 nm) inside ZnO particles [20]. Furthermore, the isotherm shows a hysteresis at p/p_0 from 0.4 to 1, due to capillary condensation in mesopores (2–30 nm) corresponding in the voids between the 20–30 nm ZnO powder particles [20].

Finally, the specific surface area obtained by the BET method of the calcined ZnO powder is equal to 10.52758 $m^2\,g^{-1}$, characteristic of a material with low porosity, or a crystallized material [14,15].

UV–Vis spectroscopy is an effective tool to investigate the light absorbing behavior of solid powders [21]. Fig. 5 shows the UV–Vis diffuse reflectance spectra of the calcined ZnO powder. Using the method reported by Provenzano et al. [22], the absorption edge value was calculated to be 380 nm. The absorption is at < 400 nm that indicates the absorption edge active at ultra violet (UV) region.

A band gap (Eg) of ZnO powder was calculated [23] from the equation:

$$\text{Eg} = hc/\lambda = 1240/\lambda \quad \text{(II)}$$

where h is plank constant = 6.626×10^{-34} J s, c is speed of light = 2.998×10^8 ms^{-1}, λ is cutoff wavelength at 380 nm corresponding to the band gap of 3.263 eV.

Because one of the aims of this work is to determine the influence of pH on the photocatalytic activity of photocatalyst,

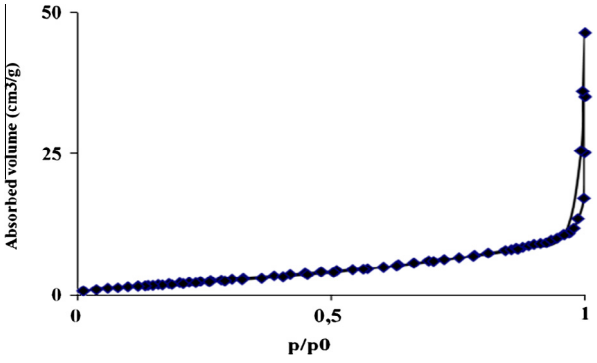

Figure 4 Nitrogen adsorption–desorption isotherm of the calcined ZnO powder.

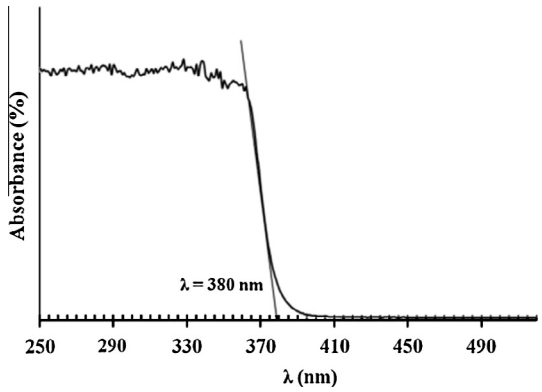

Figure 5 UV–Vis spectra of calcined ZnO powder.

it is very important to know the pH_{PZC} of the calcined ZnO powder. The pH_{PZC} of the calcined ZnO powder is shown in Fig. 6. The pH_{PZC} is the point where the curve of pH_{final} vs. $pH_{initial}$ intersects the line $pH_{initial} = pH_{final}$, with the value for the calcined ZnO powder being 8.6.

3.2. Photocatalytic activity of the calcined ZnO powder

Photodegradation experiments were carried out under the following conditions: (i) irradiation of phenol and benzoic acid solutions (0.1 g L^{-1}) under UV light in the absence of ZnO (ii) irradiation of phenol and benzoic acid solutions (0.1 g L^{-1}) with ZnO ([ZnO] = 1.0 g L^{-1}) in dark, and (iii) irradiation of phenol and benzoic acid solutions (0.1 g L^{-1}) under UV light in the presence of ZnO ([ZnO = 1.0 g L^{-1}]). The results of the studies as given in Figs. 7a and 7b show that direct photolysis did not cause any significant degradation under UV irradiation. In the presence of ZnO without irradiation, slight loss was observed due to the adsorption of phenol and benzoic acid on the surface of ZnO. The irradiation under UV light in the presence of catalyst caused 69.75% degradation of phenol and 67.98% degradation of benzoic acid in 120 min.

3.3. Effect of initial pH

The pH values of the different wastewaters are different, and they influence the photocatalytic reactions for removal of the pollutants [24]. Figs. 8a and 8b is shown the photodegradation of phenol and benzoic acid in contact with the calcined ZnO powder as a function of time with following operating variables: three different pH values for the phenolic solution (2.5, 6.5, and 12.5), [ZnO] = 1 g L^{-1} and C_0 = 0.1 g L^{-1}. The degradation rate of both substrates is maximum at acidic pH and decreased with increasing pH. The observed trends are clearly correlated with the electrostatic interactions between the substrate and the photocatalyst surface, depending on the pH of the suspension [25]. This phenomenon was caused by the surface properties of photocatalyst. The point of zero charge (pH_{pzc}) of ZnO powder is about pH 8.60. Above this pH value, the surfaces of ZnO particles are negatively charged, while below this pH value, they are positively charged [26]. Some ionic compounds such as phenolate and benzoate having negative charges could be adsorbed on the surfaces of ZnO

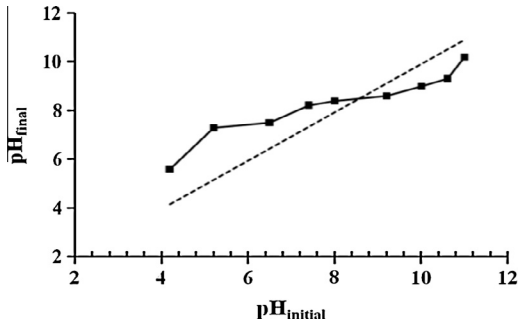

Figure 6 PZC determination of the calcined ZnO powder.

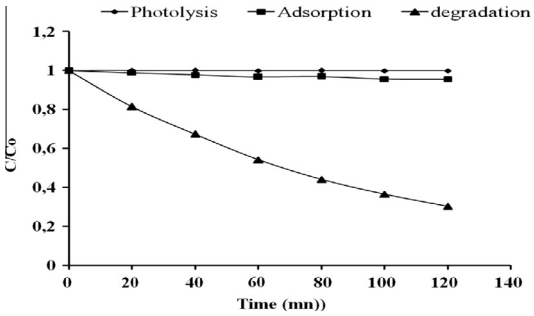

Figure 7a Removal efficiency of phenol at: [phenol] = 0.1 g L^{-}[ZnO] = 1.0 g L^{-1}.

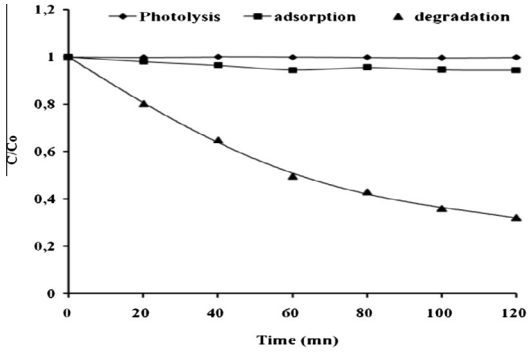

Figure 7b Removal efficiency of benzoic acid at: [benzoic acid] = 0.1 g L^{-}[ZnO] = 1.0 g L^{-1}.

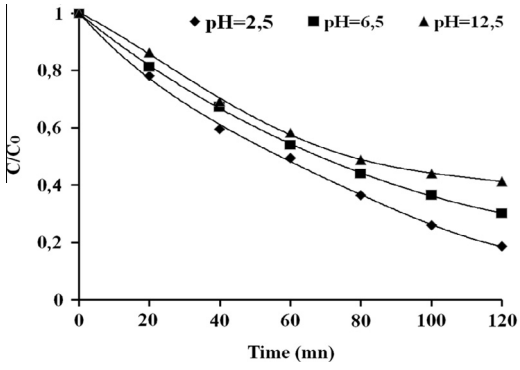

Figure 8a Effect of pH on photocatalytic degradation of phenol. [ZnO] = 1.0 g L^{-1}, $[phenol]_0$ = 0.1 g L^{-1}.

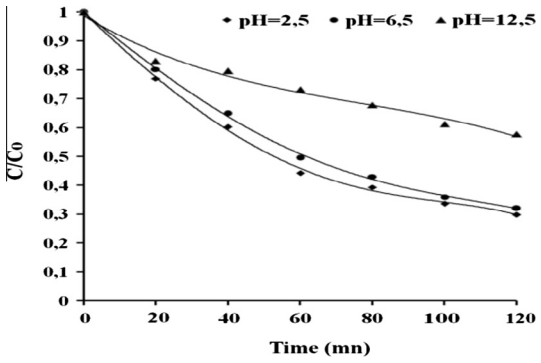

Figure 8b Effect of pH on photocatalytic degradation of phenol. [ZnO] = 1.0 g L^{-1}, [benzoic acid]$_0$ = 0.1 g L^{-1}.

particles easily below its pH_{pzc}, while phenolate and benzoate anions are repelled from the negatively charged photocatalyst surface at pH above the pHzpc of ZnO, according to a simple surface charge model [13].

3.4. Effect of the amount of ZnO

In order to avoid an ineffective excess of catalyst and to ensure a total absorption of efficient photons, the optimum mass of the calcined ZnO powder photocatalyst needs to be found. Experiments were carried out taking different amounts of ZnO, keeping the dye concentration constant (mg L^{-1}). Fig. 9 illustrates the effect of different amounts (0.5–2.5 g L^{-1}) of calcined ZnO powder on the decomposition of the phenol and benzoic acid molecules. It is clear from Fig. 9 that the degradation rate of both substrates increases with an increase in the mass of catalyst up to an amount of 1.5 g L^{-1}. An increase in the degradation rate is due to an increase in the number of active sites on ZnO available for the reaction, which in turn increases the rate of radical formation. The reduction in the rate constant may be due to the reduction in the penetration of light with surplus amount of ZnO. The surplus addition of the catalyst makes the solution more turbid and light penetration is retarded. The addition of surplus catalyst also results in the deactivation of activated molecules by collision with ground state molecules [27].

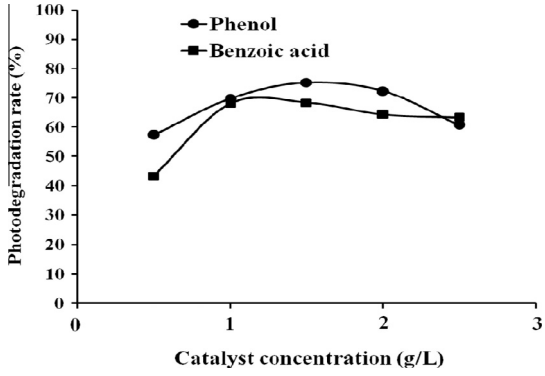

Figure 9 Effect of ZnO concentration. pH = 6.50, [phenol]$_0$ = [benzoic acid]$_0$ = 0.1 g L^{-1}.

3.5. Effect of initial concentration of phenol and benzoic acid

It is well known that the initial concentration of reactant plays an important role on the photodegradation of organic compounds [28]. The degradation rate decreases with increasing initial concentration. Similar results are shown on the photocatalytic degradation of various organic compounds [29]

The initial phenol and benzoic acid concentrations, C_0, were varied from 0.05 to 0.25 g L^{-1} at pH = 2.5 and with [ZnO] = 1.0 g L^{-1}. Figs. 10a and 10b show, respectively, the effect of initial concentration of phenol and benzoic acid on their photocatalytic degradation. It is observed that $(C/C_0)_{120}$ slightly decreases when C_0 increases from 0.05 to 0.20 g L^{-1}. This behavior can be due to an increment of adsorbed compounds on the photocatalyst surface, which is followed by their degradation. We note that $(C/C_0)_{120}$ begins to increase when C_0 is increased to 0.25 g L^{-1}. This observation is in agreement with previous studies [30–32], as phenol and benzoic acid concentration increases, more reaction intermediates are adsorbed on the surface of the photocatalyst. Therefore, these by-products compete with phenol and benzoic acid for adsorption sites on the surface of ZnO, and the degradation of both substrates is slowed down.

3.6. Kinetic studies of phenol and benzoic acid degradation in ZnO/UV process

The photocatalytic oxidation kinetics of many organic compounds has often been modeled with the Langmuir–Hinshelwood equation, which also covers the adsorption properties of the substrate on the photocatalyst surface [33]. This model, developed by [34,35], is expressed by the equation:

$$r = -\frac{dC}{dt} = K_{app}C \qquad \text{(III)}$$

where r is the degradation rate (mg/L min), K_{app} the apparent constant of degradation (1/min), C is the concentration of the organic substrate at any time t (mg/L).

The integration of this equation (with limitation: $C = C_0$ for $t = 0$) leads to the following equation:

$$\mathrm{Ln}\frac{C_0}{C} = K_{app}t \qquad \text{(IV)}$$

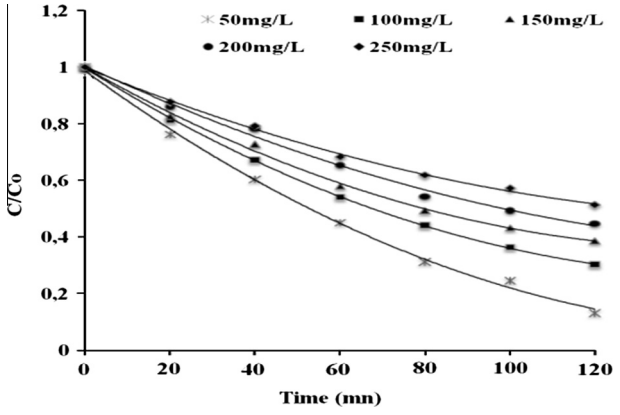

Figure 10a Effect of initial concentration of phenol on the photocatalytic degradation under UV light illumination.

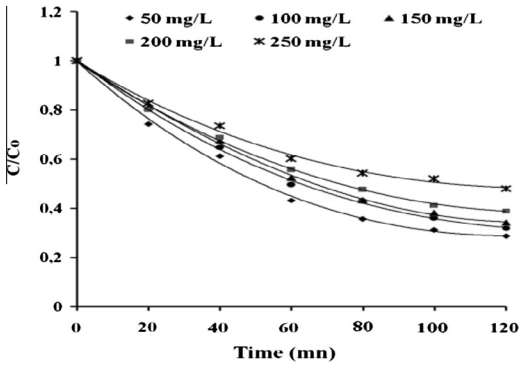

Figure 10b Effect of initial concentration of benzoic acid on the photocatalytic degradation under UV light illumination.

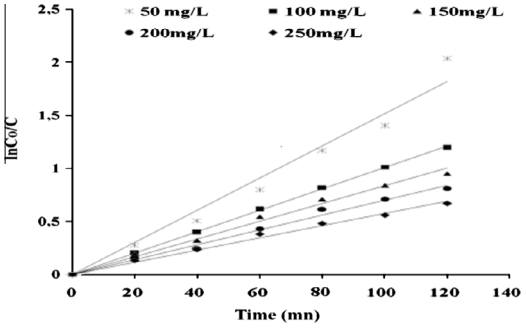

Figure 11a Kinetic fit for the degradation of phenol with ZnO. [ZnO] = 1.0 g L^{-1}; pH = 6.5.

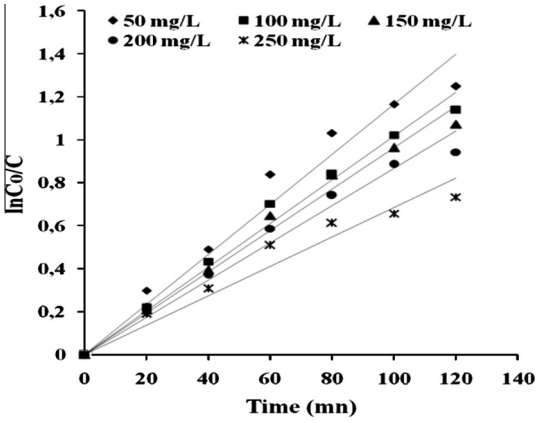

Figure 11b Kinetic fit for the degradation of benzoic acid with ZnO. [ZnO] = 1.0 g L^{-1}; pH = 6.5.

A plot of Ln $\frac{C_0}{C}$ vs. time represents a straight line, the slope of which upon linear regression equals the apparent first-order rate constant K_{app}.

The kinetics of disappearance of phenol and benzoic acid at different concentrations is respectively illustrated in Figs. 11a and 11b. The results show that the photocatalytic degradation of both compounds can be described by the first-order kinetic model. The plots of the concentration data gave a straight line. The correlation constant for the fitted line and the rate constants are calculated and their values are grouped in Table 1.

Table 1 Rate constants for catalytic photodegradation of phenol and benzoic acid.

Phenol			Benzoic acid		
C_i (mg/L)	R^2	K_{app}	C_i	R^2	K_{app}
50	0.971	0.015	50	0.958	0.011
100	0.996	0.01	100	0.984	0.010
150	0.990	0.008	150	0.983	0.009
200	0.990	0.007	200	0.973	0.008
250	0.992	0.005	250	0.947	0.006

4. Conclusions

The sol–gel process used in this work allowed producing a crystalline pure ZnO powder after a calcinations step. This calcined ZnO powder was very active for the degradation of phenol and benzoic acid under UV irradiation.

The photocatalytic degradation of various toxic organic compounds has been proposed as a viable process to detoxify aquatic solutions.

The photocatalytic process was influenced by several operating variables such as pH of the solution, catalyst loading and initial phenol and benzoic acid concentrations. In this work, it was established that the use of a pH = 2.5 for the medium, a ZnO concentration = 1.5 g L^{-1} and initial phenol concentration = 0.20 g L^{-1} allowed the degradation of about 60% of phenol after 120 min.

These first results being interesting, the degradation of phenol and benzoic acid by-products, such as catechol and hydroquinone, are actually studied on ZnO photocatalyst synthesized by the sol–gel process. In parallel, the sensitization of ZnO under visible light is developed by doping with alkaline elements such as Li, Na, and K.

References

[1] F. Delval, G. Crini, J. Vebrel, Removal of organic pollutants from aqueous solutions by adsorbents prepared from an agroalimentary by-product, Bioresour. Technol. 97 (16) (2006) 2173–2181.
[2] M.A. Fox, M.T. Dulay, Heterogeneous photocatalysis, Chem. Rev. 93 (1993) 341–357.
[3] M.R. Hoffmann, S.T. Martin, W. Choi, D. Bahnemann, Environmental applications of semiconductor photocatalysis, Chem. Rev. 95 (1) (1995) 69–96.
[4] A. Fujishima, T.N. Rao, D.A. Tryk, Titanium dioxide photocatalysis, J. Photochem. Photobiol., C 1 (2000) 1–21.
[5] A. Fujishima, K. Honda, Electrochemical photolysis of water at a semiconductor electrode, Nature 238 (5358) (1972) 37–38.
[6] Benito Serrano Rosales, I.Hugo de Lasa, Aaron Ortiz, Miguel Salaices, Quasi equilibrium and non-equilibrium adsorption in heterogeneous photocatalysis, Chem. Eng. Sci. 62 (2007) 5160–5166.
[7] V. Dijken, A.H. Janssen, M.H.P. Smitsmans, D. Vanmaekelbergh, K. Meijerink, Size-selective photoetching of nanocrystalline semiconductor particles, Chem. Mater. 10 (11) (1998) 3513–3522.
[8] B. Neppolian, S. Sakthivel, M. Palanichamy, Banumathi Arabindoo, V. Murugesan, Degradation of textile dye by solar light using TiO_2 and ZnO photocatalysts, J. Environ. Sci. Health Part-A A 34 (9) (1999) 1829.

Please cite this article in press as: H. Benhebal et al., Photocatalytic degradation of phenol and benzoic acid using zinc oxide powders prepared by the sol–gel process, Alexandria Eng. J. (2013), http://dx.doi.org/10.1016/j.aej.2013.04.005

[9] C. Shifu, Z. Wei, Z. Sujuan, L. Wei, Preparation, characterization and photocatalytic activity of N-containing ZnO powder, Chem. Eng. J. 148 (2009) 263–269.
[10] C.J. Brinker, G.W. Scherer, Sol–gel science: the physics and chemistry of sol–gel processing, Academic Press, San Diego, 1990.
[11] S. Lambert, L. Sacco, F. Ferauche, B. Heinrichs, A.F. Noels, J.-P. Pirard, Synthesis of SiO_2 xerogels and Pd/SiO_2 cogelled xerogel catalysts from silylated acetylacetonate ligand, J. Non-Cryst. Solids 343 (2004) 109–120.
[12] J.Céline Bodson, D. Stéphanie, Christelle Alié, Xavier Cattoën, Jean-Paul Pirard, Catherine Bied, Michel Wong Chi Man, Benoît Heinrichs, Effects of additives and solvents on the gel formation rate and on the texture of P- and Si-doped TiO_2 materials, Micropor. Mesopor. Mater. 134 (2010) 157–164.
[13] M. Mrowetz, E. Selli, Photocatalytic degradation of formic and benzoic acids and hydrogen peroxide evolution in TiO_2 and ZnO water suspensions, J. Photochem. Photobiol., A 180 (2006) 15–22.
[14] B. Braconnier, C. Paez, S. Lambert, C. Alié, C. Henrist, D. Poelman, J.-P. Pirard, R. Cloots, B. Heinrichs, Ag- and SiO_2-doped porous TiO_2 with enhanced thermal stability, Micropor. Mesopor. Mater. 122 (2009) 247–254.
[15] C.A. Paez, D. Poelman, J.-P. Pirard, B. Heinrichs, Unpredictable photocatalytic ability of H_2-reduced rutile-TiO_2 xerogel in the degradation of dye-pollutants under UV and visible light irradiation, Appl. Catal. B 94 (2010) 263–271.
[16] M.V. Lopez-Ramon, F. Stoeckli, C. Moreno-Castilla, F. Carrasco-Marin, On the characterization of acidic and basic surface sites on carbons by various techniques, Carbon 37 (1999) 1215–1221.
[17] E.A. Clesceri, A. Greenberg, Standard Methods for Examination of Water and Wastewater, 19th ed., APHA, AWWA and WEF, Washington, DC, 1995.
[18] Lei Yang, Guozhong Wang, Chunjuan Tang, Hongqiang Wang, Lide Zhang, Synthesis and photoluminescence of corn-like ZnO nanostructures under solvothermal-assisted heat treatment, Chem. Phys. Lett. 409 (2005) 337–341.
[19] A.R. West, Solid State Chemistry and its Application, Wiley, New York, 1984.
[20] A.J. Lecloux, in: J.R. Anderson, M. Boudart (Eds.), Catalysis: Science and Technology, vol. 2, Springer, Berlin, 1981, p. 171.
[21] Haiyan Jiang, Hongxing Dai, Yunsheng Xia, Hong He, Synthesis and characterization of wormhole-like mesoporous SnO_2 with high surface area, Chin. J. Catal. 31 (2010) 295–301.
[22] P.L. Provenzano, G.R. Jindal, J.R. Sweet, W.B. White, Flame-excited luminescence in the oxides Ta_2O_5 Nb_2O_5 TiO_2 ZnO and SnO_2, J. Lumin. 92 (2001) 297–305.
[23] B. O'Regan, M. Gratzel, A low-cost, high-efficiency solar cell based on dye sensitized colloidal TiO_2 films, Nature 353 (1991) 737–740.
[24] Wei Liu, Shifu Chen, Wei Zhao, Sujuan Zhang, Study on the photocatalytic degradation of trichlorfon in suspension of titanium dioxide, Desalination 249 (2009) 1288–1293.
[25] D.H. Kim, M.A. Anderson, Solution factors affecting the photocatalytic and photoelectrocatalytic degradation of formic acid using supported TiO_2 thin films, J. Photochem. Photobiol. A: Chem. 94 (1996) 221–229.
[26] Jun Wang, Zhe Jiang, Zhaohong Zhang, Yingpeng Xie, Xiaofang Wang, Zhiqiang Xing, Xu Rui, Xiangdong Zhang, Sonocatalytic degradation of acid red B and rhodamine B catalyzed by nano-sized ZnO powder under ultrasonic irradiation, Ultrason Sonochem. 15 (5) (2008) 768–774.
[27] A.K. Subramani, K. Byrappa, S. Ananda, K.M. Lokanatha Rai, C. Ranganathaiah, M. Yoshimura, Photocatalytic degradation of indigo carmine dye using TiO_2 impregnated activated carbon, Bull. Mater. Sci. 30 (2007) 37–41.
[28] R.W. Matthews, Photooxidation of organic impurities in water using thin films of titanium dioxide, J. Phys. Chem. 91 (1987) 3328.
[29] V. Augugliaro, L. Palmisano, M. Schiavello, A. Sclafani, L. Marchese, G. Martra, F. Miano, Photocatalytic degradation of nitrophenols in aqueous titanium dioxide dispersion, Appl. Catal. 69 (1991) 323–340.
[30] L. Zhang, T. Kanki, N. Sano, A. Toyoda, Pathways and kinetics on photocatalytic destruction of aqueous phenol, Environ. Monit. Assess. 115 (2006) 395–403.
[31] C.G. Silva, J.L. Faria, Effect of key operational parameters on the photocatalytic oxidation of phenol by nanocrystalline sol–gel TiO_2 under UV irradiation, J. Mol. Catal. A 305 (2009) 147–154.
[32] R. Singla, M. Ashokkumar, F. Grieser, The mechanism of the sonochemical degradation of benzoic acid in aqueous solutions, Res. Chem. Intermed. 30 (2004) 723–733.
[33] N.A. Laoufi, D. Tassalit, F. Bentahar, The degradation of phenol in water solution by TiO_2 photocatalysis in a helical reactor, Global NEST J. 10 (2008) 404–418.
[34] C.S. Turchi, D.F. Ollis, Photocatalytic degradation of organic water contaminants; mechanisms involving hydroxyle radical attack, J. Catal. 122 (1990) 178–192.
[35] A.V. Emeline, V. Ryabchuk, N. Serjone, Factors affecting the efficiency of a photocatalysed process in aqueous metal-oxide dispersions, prospect of distinguishing between two kinetic models, J. Photochem. Photobio. A: Chem. 133 (2000) 89–97.

Please cite this article in press as: H. Benhebal et al., Photocatalytic degradation of phenol and benzoic acid using zinc oxide powders prepared by the sol–gel process, Alexandria Eng. J. (2013), http://dx.doi.org/10.1016/j.aej.2013.04.005